Synthesis of oil-laden poly(ethylene glycol) diacrylate hydrogel nanocapsules from double nanoemulsions

*Mengwen Zhang, Maksymilian Nowak, Paula Malo de Molina, Michael Abramovitch, Katherine Santizo, Samir Mitragotri, Matthew E. Helgeson**

Department of Chemical Engineering, University of California, Santa Barbara, California 93106, United States

* helgeson@engineering.ucsb.edu

ABSTRACT Multiple emulsions have received great interest due to their ability to be used as templates for the production of multi-compartment particles for a variety of applications. However, scaling these complex droplets to nanoscale dimensions has been a challenge due to limitations on their fabrication methods. Here, we report the development of oil-in-water-in-oil ($O_1/W/O_2$) double nanoemulsions *via* a two-step high-energy method, and their use as templates for complex nanogels comprised of inner oil droplets encapsulated within a hydrogel matrix. Using a combination of characterization methods, we determine how the properties of the nanogels are controlled by the size, stability, internal morphology, and chemical composition of the nanoemulsion templates from which they are formed. This allows for identification of

compositional and emulsification parameters that can be used to optimize the size and oil encapsulation efficiency of the nanogels. Our templating method produces oil-laden nanogels with high oil encapsulation efficiencies and average diameters of 200-300 nm. In addition, we demonstrate the versatility of the system by varying the types of inner oil, the hydrogel chemistry, the amount of inner oil, and the hydrogel network crosslink density. These non-toxic oil-laden nanogels have potential applications in food, pharmaceutical, and cosmetic formulations.

KEYWORDS: double nanoemulsions; nanogel; nanoparticles; oil-in-water-in-oil; templates

INTRODUCTION

In recent years, there has been growing interest in the engineering of multiple emulsions – i.e., multi-phase droplets with internal liquid structure – and their use as templates to synthesize microparticles with complex architectures for various applications including foods,[1–4] pharmaceuticals,[5–10] cosmetics[11–13] and chemical separations.[14–16] In particular, using this approach to create multiphasic nanogel particles holds great promise in fields such as drug delivery,[17,18] cataylsis,[19] and photonics.[20]

In the case of drug delivery, the ability to co-encapsulate high concentrations of hydrophobic an hydrophilic actives within the same particle provides the possibility of delivering combinations of active therapeutic agents with disparate polarities.[21,22] While several techniques exist to encapsulate hydrophobic actives (*e.g.*, PLGA nanoparticles) and hydrophilic actives (*e.g.*, hydrogels) into nanoparticles independently, it has proven challenging to encapsulate both types of actives into a single nanoparticle while maintaining their nanoscopic size, which is

necessary for intravenous injection. Furthermore, previous multiple emulsion methods to create multi-phasic hydrogel particles produce particles with sizes at the micron-scale or larger, which restricts their use to predominantly non-intravenous routes.[23] For other applications, including foods and consumer products, this size range is also necessary for colloidal stability, *i.e.*, where Brownian motion of droplets and particles becomes sufficient to stabilize them against sedimentation. The change of particle scale from micro- to nano- is not a straightforward matter of size reduction, and therefore represents a significant technological challenge given the complexity of the internal architecture of these nanoparticles.

Although many have used simple one-phase nanoemulsions as templates for producing nanoparticles,[18,24,25] making complex emulsions on the nanoscale using existing methods has also proven to be a challenge, and using them to template particles consequently more difficult. Multiple emulsion preparation methods have included microfluidic or microcapillary-based approaches[22,26–32] and bulk emulsification methods.[33–37] While microcapillary-based methods offer precise control over droplet sizes and distribution, they have low throughput (typically less than 1 mL/hr for a single device[38]), and device limitations make nanoscale droplet production infeasible without significant technological advances. On the other hand, bulk emulsification has been used to successfully form nanoscale multiple emulsions, but is significantly more difficult to control, typically resulting in a large dispersity of both size and morphology. More innovative approaches such as one-step preparation of multiple emulsions using amphiphilic block copolymers or induced by phase separation have improved controllability in both droplet size and morphology; however, scaling them down to the nanoscale remains challenging.[38] Here, we choose a two-step, high-energy bulk emulsification method. The method is inherently scalable due to the availability of industrial high-energy emulsification equipment.[39,40] It is versatile in

that it can be adapted to a wide range of oils, aqueous phases and surfactants. Finally, it provides relatively simple control over the composition of the inner and outer droplet phases to tailor to specific applications and needs.

There have been only a few reports of double and complex nano-scale emulsions with well-specified morphology to date; of these, most examples consist of water-oil-water (W/O/W) double nanoemulsions, in which the inner aqueous droplets are stabilized in oil globules, which are further suspended in an external aqueous phase.[41–45] Zhao *et al*. induced the formation of W/O/W double nanoemulsions in a cetyltrimethylammonium bromide (CTAB)/water/heptane mixture by introducing compressed CO_2 into the system, and demonstrated their use as templates for hollow silica nanoparticles.[44] Shakeel *et al.* created a double W/O/W nanoemulsion via spontaneous emulsification to deliver 5-fluorouracil for cancer therapy.[41] Lee at al. were able to produce complex structured nanoemulsions using a mixture of surfactants and cosurfactants.[42,45]

Alternatively, the templating of hydrogel nanoparticles within emulsions requires the opposite emulsion structure, i.e. O/W/O nanoemulsions. However, compared to W/O/W double nanoemulsions, literature on the formation of O/W/O double nanoemulsions is even more limited. Recently, we demonstrated the formation of O/W/O nanoemulsions using a one-step emulsification method by employing a judicious choice of co-surfactants.[43] However, this one-step method is likely incompatible with situations where the desired inner oil phase is distinct from the outer oil. In addition, this technique is limited to making vesicle-type structures with swollen water films, and therefore cannot create structures where many small droplets are suspended in a larger droplet.

To address this need, we herein report a simple 2-step sequential emulsification method for the preparation of $O_1/W/O_2$ double nanoemulsions. We analyze the stability of these emulsions, as well as feasible operating conditions that demonstrate their capability to be used as templates for forming nanogels with complex structures and encapsulated nanodroplet phases.

RESULTS AND DISCUSSION

Production of single O_1/W and W/O_2 nanoemulsions

The desired multiple nanoemulsions sought in this work comprise an inner oil nanodroplet phase (O_1) encapsulated within nanodroplets of a dispersed aqueous phase (W) containing a photocrosslinkable hydrogel pre-cursor, poly(ethylene glycol) diacrylate (PEGDA), which are suspended within an outer oil phase (O_2). For most studies, a high-viscosity silicone oil phase was chosen as a model chemistry for the O_1 phase due to its relatively low solubility in water/PEGDA mixtures.[21] PEGDA (M_n = 700 g/mol) was the polymer of choice for most studies due to its high water solubility, relatively fast polymerization kinetics, ability to crosslink with itself to form hydrogels, and biocompatibility. Based on our previous studies of the production of O/W/O multiple nanoemulsions,[43] we chose cyclohexane as the O_2 phase due to its low viscosity and relative volatility (to facilitate separation), and a mixture of conventional ethoxylated nonionic surfactants Span80, Tween80, and Tween20 due to their ability to form stable nanoemulsions.[46]

Single oil-in-water (O_1/W) nanoemulsions were formed by ultrasonicating a coarse emulsion composed of silicone oil (O_1) in an aqueous PEGDA solution containing Tween20 surfactant. When keeping the composition constant, the final size of the nanoemulsion can be controlled by adjusting either the power or time of ultrasonication.[47,48] In the canonical

composition, 10 vol% of the total suspension volume was silicone oil (Φ^{O_1} = 0.10), 33 vol% of the aqueous phase volume was PEGDA (ϕ^{W}_{PEGDA} = 0.33), with the surfactant, Tween20, being at a concentration of 100 mM in the aqueous phase (C^{W}_{T20} = 100 mM). For nanoemulsions with this composition, average sizes measured by dynamic light scattering (DLS) range from approximately 30-400 nm depending on the ultrasonication power and processing time (Figure 1b). The average droplet size decreases as more mechanical energy is added to the system until a size plateau is reached, whereby the deformations applied to the fluid are no longer sufficient to break up the droplets.[47] These droplet sizes are corroborated by cryo-TEM (Figure 1a). The stability of the nanoemulsions was determined by measuring the droplet size over time (Figure 1c). As expected for nanoemulsions of such a small size,[47,49] these droplets are extremely stable, with no appreciable change in diameter over multiple months (Figure 1c).

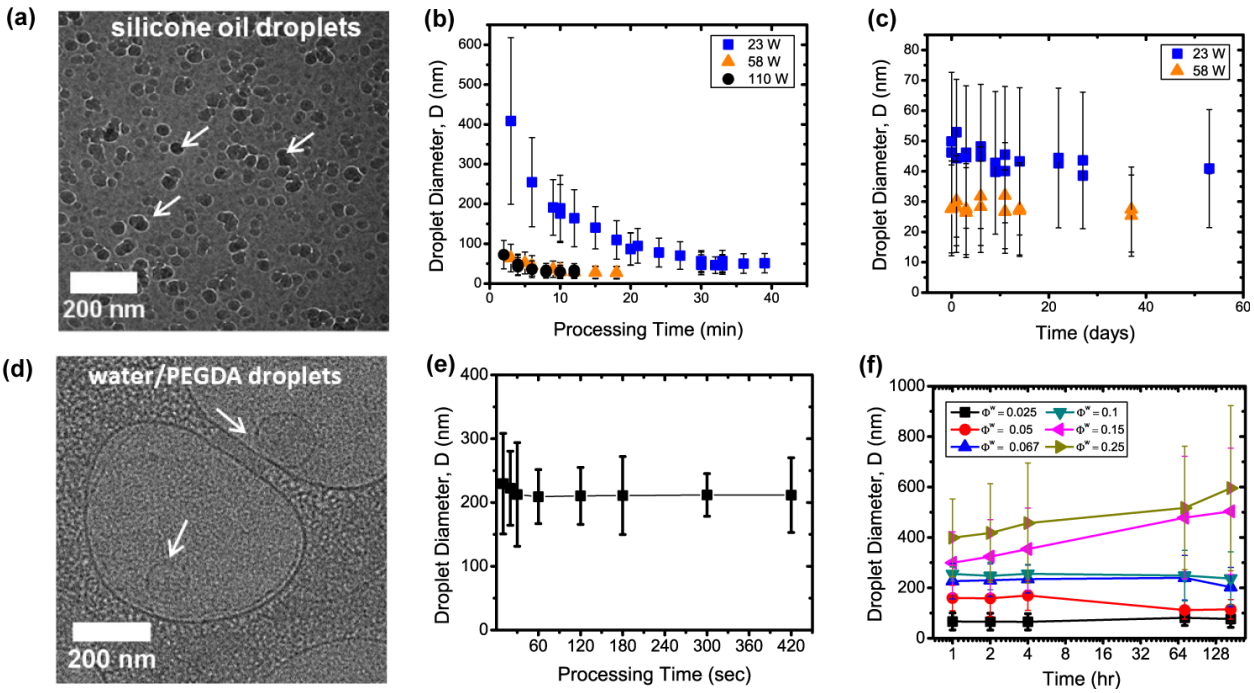

Figure 1. (a) Cryo-TEM image showing (a) an O_1/W nanoemulsion with Φ^{O_1} = 0.10 silicone oil-in-water/PEGDA and ϕ^{W}_{PEGDA} = 0.33. (b) Influence of ultrasonication time and power on the size of O_1/W nanoemulsions. (c) Stability of O_1/W nanoemulsion over a period of 2 months. (d) Cryo-TEM of Φ^{W} =

0.06 water/PEGDA-in-cyclohexane (W/O_2) nanoemulsion (sonication power = 46 W). (e) Influence of ultrasonication time on the size of $\Phi^W = 0.06$ W/O_2 nanoemulsions (power = 46 W). (f) Effect of dispersed phase volume fraction (Φ^W) in cyclohexane on nanoemulsion size and stability. The average PDI is between 0.15 to 0.25 for all samples; error bars indicate standard deviation (σ) of the droplet size distribution, where $PDI = \left(\frac{\sigma}{D}\right)^2$.

Single W/O_2 nanoemulsions were formed by ultrasonication of a coarse emulsion of hydrogel precursor solution in cyclohexane with Span80 and Tween80 as co-surfactants, similar to a system used in previous work to generate uniform nanogel particles.[25,43] As a canonical composition, the dispersed W phase composed of 33 vol% PEGDA (ϕ^W_{PEGDA} = 0.33) and water was emulsified cyclohexane containing Span80 and Tween80 ($C^{O_2}_{T80}$= 5mM, $C^{O_2}_{S80}$ = 47 mM) to achieve a final dispersed phase volume fraction of Φ^W = 0.06. Cryo-TEM shows distinct 100 nm to 200 nm droplets dispersed in cyclohexane (Figure 1d). The effect of ultrasonication time on W/O_2 nanoemulsion size was measured *via* DLS and exhibited a trend qualitatively similar to that of the O_1/W nanoemulsion (Figure 1e). As with the O_1/W nanoemulsion, this trend is a result of additional energy input, which breaks up the emulsion into progressively smaller droplets combined with mechanical limitations on the minimum droplet size.[47] The aqueous phase volume fraction (Φ^W) provides some degree of control over the droplet size over a relatively wide range, with final droplet sizes ranging from 70 nm to over 400 nm (Figure 1f). Droplet size was then monitored over time with DLS. Larger droplets ($\geq \Phi^W$=0.15) showed limited stability, but the smaller sizes remained stable for multiple weeks (Figure 1f), demonstrating that smaller W/O_2 nanoemulsions possess adequate stability for particle templating.

Synthesis of oil-laden nanogels from $O_1/W/O_2$ double nanoemulsion templates

Having demonstrated the capability of controlling both the size and stability of the single O_1/W and W/O_2 nanoemulsions, we attempted the creation of $O_1/W/O_2$ double nanoemulsions,

and subsequently PEGDA nanogels templated from them. To do so, we employed a serial nanoemulsification protocol, in which an oil-in-water (O_1/W) nanoemulsion is prepared by ultrasonication, and then itself emulsified into an outer oil (O_2) phase *via* a second ultrasonication process (Figure 2a). Detailed compositions can be found in Table S1 of the ESI. After the addition of photo-initiator and exposure to UV light, the PEGDA in the O_1/W/O_2 double nanoemulsion is photo-polymerized and forms oil-laden nanogels. The nanogels are subsequently purified and stored in DI water at 10° C in order to minimize oil solubility in the continuous phase. The amount of oil loss during storage over a period of 40 days is negligible once the nanogels have been crosslinked (Table S2), due to the considerable droplet stability of nanoemulsions compared to micron-sized droplets.[47]

Cryo-TEM images for several important steps were acquired to aid visualization of the synthesis process (Figure 2a). Figure 2b shows a representative cryo-TEM image of a typical O_1/W/O_2 double nanoemulsion, i.e., a silicone oil-in-water/PEGDA-in-cyclohexane nanoemulsion. We observe circular 20-30 nm darker features indicating droplets encapsulated in larger droplets of lower average intensity that have distinct thin edges surrounding them, indicating the surfactant layer. Combined with the DLS measurements of the O_1/W and W/O_2 simple nanoemulsions, this confirms the encapsulation of silicone oil droplets with an average diameter of 30 nm in hydrogel precursor droplets with an average diameter of 300 nm.

The image in Figure 2c was acquired after the addition of photo-initiators and exposure to UV light, which initiates polymerization of the water/PEGDA phase of the double nanoemulsion. Again, we observe structures and contrast resembling those in Figure 2b with the only difference being the disappearance of thin rings around the 300 nm water/PEGDA droplets. This can be attributed to the disruption of the surfactant layer as the PEGDA polymerizes into a three-

dimensional hydrogel network. Finally, after purifying the nanogels through a series of centrifugation and solvent exchange processes and re-dispersing the nanogels into deionized (DI) water, we observe with more clarity the final structure of the oil-laden nanogels (Figure 2d, Figure S2). The fact that the final oil-laden nanogels retain similar structure as the initial $O_1/W/O_2$ template confirms the effectiveness of the double nanoemulsion template.

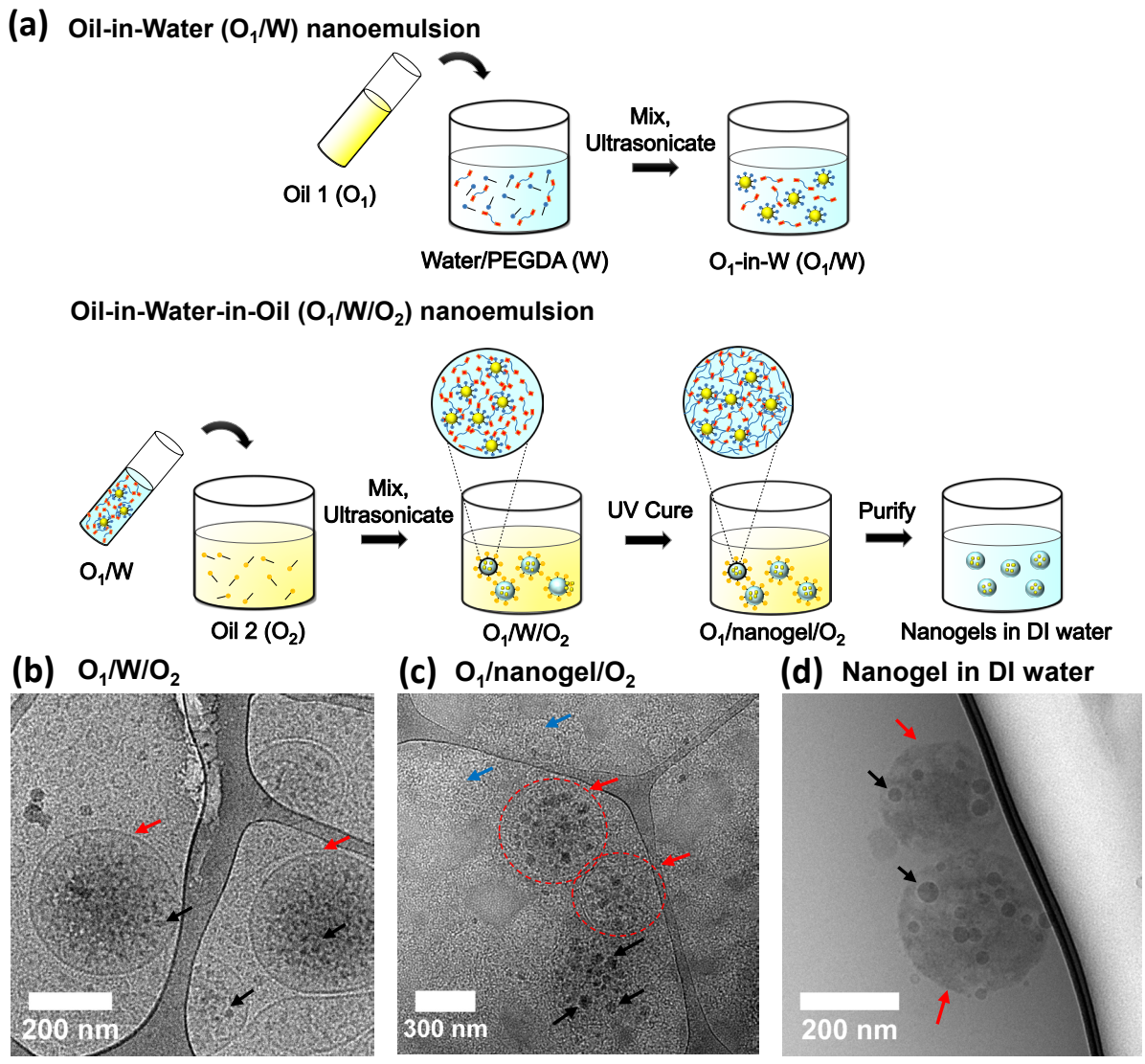

Figure 2. (a) Synthesis schematics for $O_1/W/O_2$ double nanoemulsion and templating of oil-laden nanogels. (b-d) Cryo-TEM image of silicone oil-in-water/PEGDA-cyclohexane double

nanoemulsion ($O_1/W/O_2$) ($\Phi^{O_1} = 0.04$ and $\phi^{W}_{PEGDA} = 0.25$, C^{W}_{T20} =44mM, Φ^{W} =0.06, $C^{O_2}_{T80}$=5mM, $C^{O_2}_{S80}$=47mM), polymerized nanogels in cyclohexane (O_1/nanogel/O_2), and purified oil-laden nanogels suspended in water; (red, black, blue arrows denote oil droplets, water/PEGDA droplets, and regions of beam damage, respectively).

Controlling the encapsulation efficiency of oil within oil-laden nanogels

A number of studies have reported on the dynamic instability of double emulsion droplets.[43,50–55] Unlike single emulsions, whose stability can be inferred from changes in their droplet size distribution alone, the stability of double emulsions is additionally characterized by the amount of inner droplet phase retained within the outer droplet phase, i.e., the encapsulation efficiency.[53] Most studies of encapsulation efficiency have been in W/O/W emulsions, where efficiency is typically measured either by encapsulating a water-soluble molecular probe (*e.g.* NaCl) and measuring its release profile under different compositional makeup and processing conditions, or using *in situ* microscopy to track the size distribution and amount of the inner phase.[4] Here, we instead choose a more direct, quantitative approach, whereby the choice of silicone oil as the inner oil phase facilitates direct quantification using solid-state NMR (see Methods section) both before the initial nanoemulsification process and after the resulting oil-laden nanogels have been synthesized and purified.

Figure 3 shows a representative NMR spectrum of the oil-laden nanogels. By quantifying the area of the various distinct peaks corresponding to silicone oil, Tween20, cyclohexane, and PEGDA, we compute the final composition of the gels and thereby the encapsulation efficiency of silicone oil. Cyclohexane is the outer oil phase (O_2) from the $O_1/W/O_2$ template, and is monitored in the final oil-laden nanogels to gauge i) how much cyclohexane is remaining after

the purification process, and ii) whether any cyclohexane is trapped inside the nanogels due to instability of $O_1/W/O_2$ during the emulsification process. As shown in Figure 3, a negligible amount of cyclohexane remains in the final purified nanogels and will thus be neglected in later analysis.

To better understand the stability of the $O_1/W/O_2$ double nanoemulsions, and determine operating conditions that optimize encapsulation efficiency, NMR spectra were measured across a range of several processing parameters, including the ultrasonication processing time of the $O_1/W/O_2$ double nanoemulsion, the waiting time between ultrasonication and UV-photopolymerization of $O_1/W/O_2$, the initial inner oil volume fraction Φ^{O_1} in O_1/W, and the PEGDA volume fraction ϕ_{PEGDA}^{W} in O_1/W. In all cases, the O_1 encapsulation efficiency (ε) is

$$\varepsilon = \frac{measured\ oil\ content}{initial\ oil\ content},$$

where the initial and final amounts of oil were determined by NMR (see Methods section).

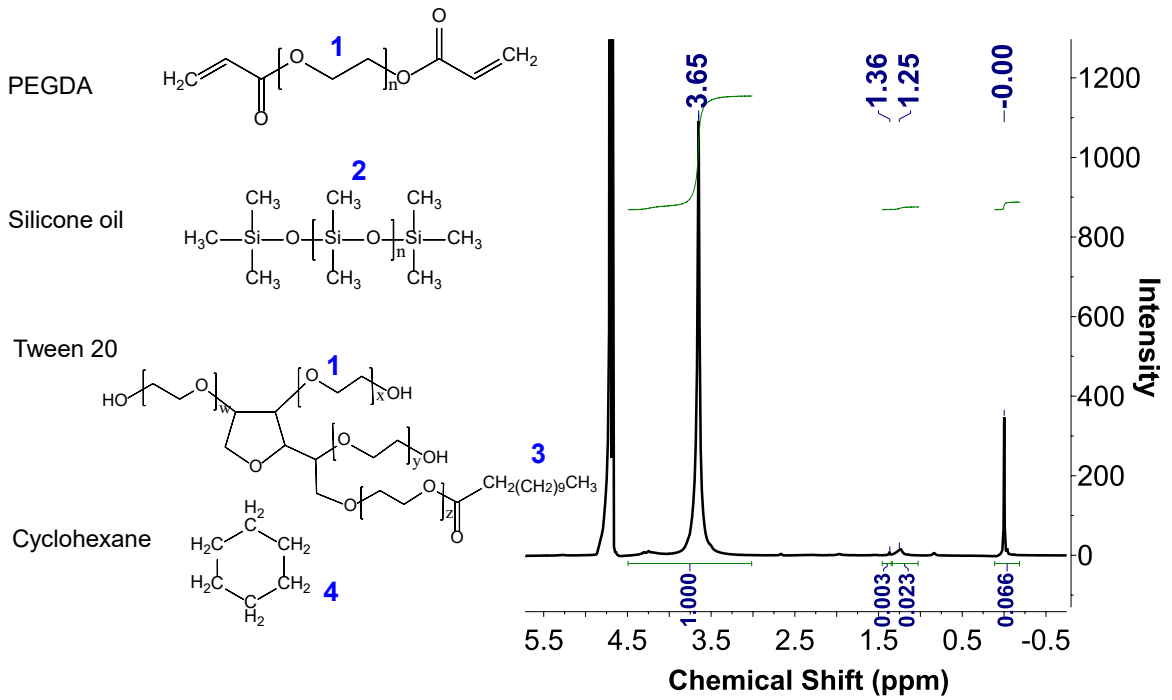

Figure 3. Representative ^{1}H-NMR spectrum for oil-laden nanogels with silicone oil as the inner oil (Φ^{O_1}=0.1), PEGDA as the crosslinkable polymer (ϕ^{W}_{PEGDA}=0.33), and Tween20 as the emulsifying surfactant in the O_1/W nanoemulsion (C^{W}_{T20} = 100mM). Any cyclohexane (O_2) retained from the O_1/W/O_2 template is monitored to check the purity of final nanogel.

These measurements were used to determine the maximum amount of inner oil (O_1) that can be encapsulated within the oil-laden nanogels. Figure 4a shows how the encapsulation efficiency (ε) and size (D_N) of nanogels change as the initial silicone oil volume fraction (Φ^{O_1}) in the O_1/W phase is systematically varied while holding the dispersed phase volume fraction (Φ^{W}), PEGDA volume fraction in the dispersed phase (ϕ^{W}_{PEGDA}), and concentration of Tween20 per oil droplet constant (ESI Section I, Table S1). Once the O_1/W nanoemulsions were prepared, 1 mL of O_1/W was added to 15 mL of cyclohexane solubilized with a surfactant mixture of 100 mg Tween80 and 300 mg Span80 ($C^{O_2}_{T80}$= 5mM, $C^{O_2}_{S80}$ = 47 mM) to formulate the O_1/W/O_2 double nanoemulsion. The double nanoemulsions were then ultrasonicated for 40 s and photocrosslinked to form nanogels.

We find that both the size polydispersity and oil content of the nanogels increase with increasing oil volume fraction from Φ^{O_1} = 0.02 to 0.10 (Figure 4a; sonication power = 32 W). For Φ^{O_1} < 0.06, the average size of nanogels ranges from 200-300 nm, with a polydispersity index (PDI) of 0.2 (reflected by the error bars in Figure 4a). However, at Φ^{O_1} = 0.10, we observe a bimodal population of droplet sizes, with a smaller population having an average size of 200 nm and a larger population having an average size of 1.0 μm. This suggests that although more oil could be encapsulated into the nanogels, it becomes difficult to control size and polydispersity for Φ^{O_1} > 0.10. We also note that the measured oil content increases linearly with increase in the initial input amount with a slope of $\varepsilon \sim 0.58$. Regardless of the input initial oil content, the oil encapsulation efficiency (ε) at each composition also decreased by approximately 40% after 40s of ultrasonication. This suggests that the mechanism responsible for oil loss is qualitatively the same regardless of initial oil content. From this, we conclude that the mechanism of oil encapsulation instability is primarily dictated by kinetic processes occurring within individual O_1/W droplets, and is only weakly influenced by interactions between dispersed O_1/W droplets.

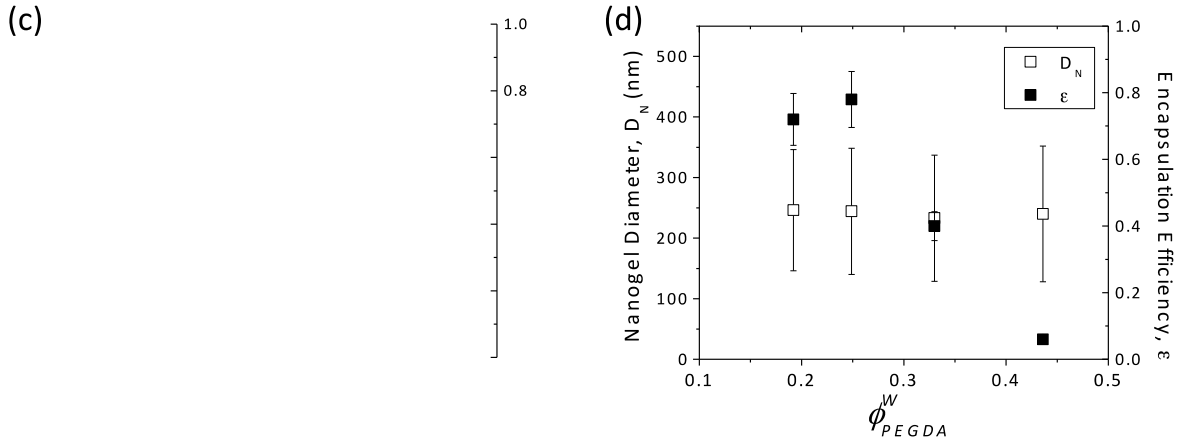

Figure 4. Effect of composition and operating parameters on oil encapsulation efficiency, (a) an increase in initial inner oil content leads to an increase in size and polydispersity of nanogels, as well as a linear increase in final oil content; (red solid, dashed lines indicate oil content assuming zero oil loss and a linear fit to the measured data). (b) Increase in ultrasonication time decreases the oil encapsulation efficiency for both Φ^{O_1} = 0.04 and Φ^{O_1} =0.10, (c) ε for nanogels with Φ^{O_1} =0.04 remains consistent for samples with varying wait time after the $O_1/W/O_2$ emulsification, (d) increase in PEGDA volume fraction decreases ε of nanogels. In (a) and (b), bimodal size distributions are indicated by the modal size of the smaller and larger populations (up and down triangles, respectively). The average PDI is between 0.15 to 0.25 for all samples; error bars indicate standard deviation (σ) of the droplet size distribution, where $PDI = \left(\frac{\sigma}{D}\right)^2$.

To further elucidate the primary mechanism for oil loss, we tested the effect of ultrasonication processing time of $O_1/W/O_2$ nanoemulsions on the final nanogel size and

encapsulation efficiency in more detail for two silicone oil volume fractions, $\Phi^{O_1} = 0.04$ and $\Phi^{O_1} = 0.10$ (Figure 4b). Detailed compositions can be located in Table S1 in ESI. For both compositions, we observe that the nanogel size and encapsulation efficiency decrease with increasing ultrasonication time. This suggests that ultrasonication plays a significant role in droplet instability, and that there is a tradeoff between size and oil encapsulation efficiency; i.e., increasing the ultrasonication time leads to smaller sizes and lower polydispersity, but at the same time reduces the oil encapsulation efficiency. This observation is demonstrated most clearly for $\Phi^{O_1} = 0.10$; in order to achieve a sufficiently small nanogel size (< 500 nm) with a narrow PDI, extensive ultrasonication is required, resulting in low oil content. Mechanistically, this suggests the kinetic stability of the O_1 phase is significantly reduced during ultrasonication of the $O_1/W/O_2$ nanoemulsion and leads to coalescence of the O_1 phase with the outer (miscible) O_2 phase. Similar results have been reported in literature for double W/O/W emulsions that exhibit destabilization due to high shear.[54] Specifically, excessive shear could induce streaming, i.e., flow within the outer droplets that induces motion of the inner droplets. In turn, this could hasten film drainage of the outer droplet fluid between the inner O_1 droplets and the W/O_2 interface, facilitating coalescence of the O_1 droplets with the outer O_2 phase (Scheme 1a). Thus, applying more moderate emulsification conditions to produce double nanoemulsions could avoid rapid reduction in encapsulation efficiency. This is likely why most of the double nanoemulsions reported previously exhibit relatively large size polydispersity.

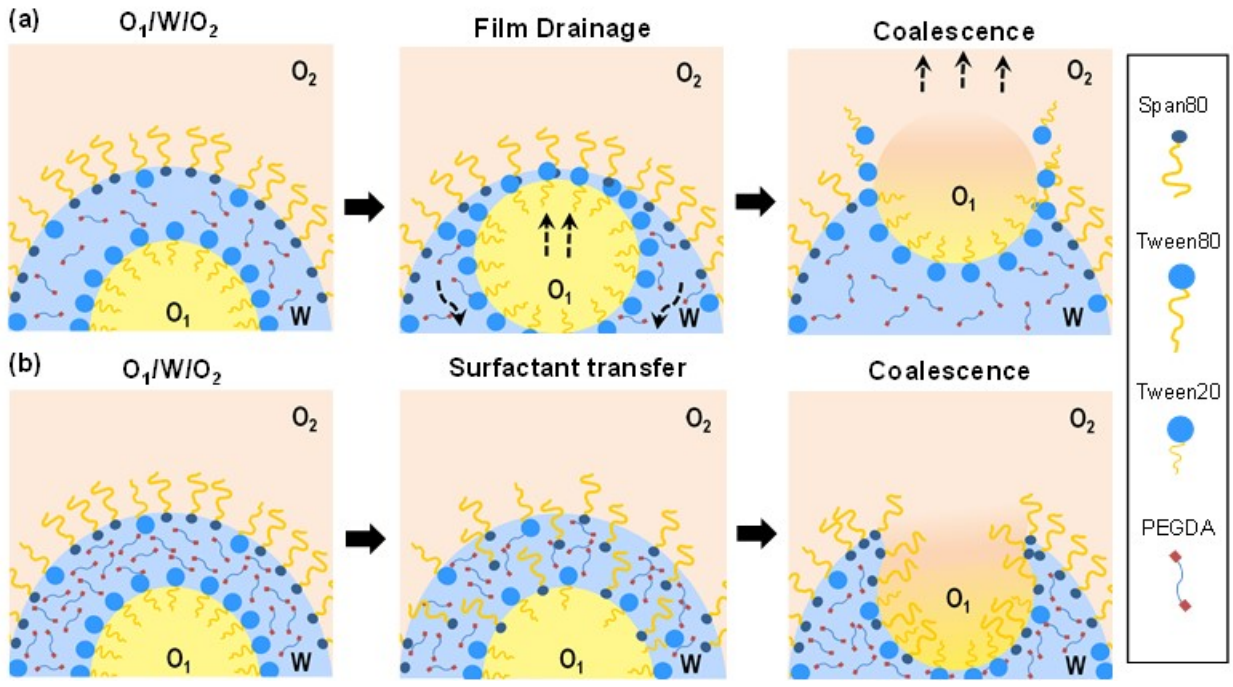

Scheme 1. Schematics showing (a) ultrasonication-induced inner droplet streaming which eventually leads to oil loss, and (b) an increase in polymer content leading to reversal of film curvature and oil loss.

To further explore the stability of the inner oil phase inside the double emulsion, we studied the dependence of the nanogel encapsulation efficiency on the waiting time between the ultrasonication step and subsequent UV-photocrosslinking of $O_1/W/O_2$ (Fig. 4c). To prepare the samples, 1 mL of O_1/W silicone oil-in-water nanoemulsion of Φ^{O_1} = 0.04, ϕ^{W}_{PEGDA}= 0.25, C^{W}_{T20} = 44 mM was added to 15 mL of cyclohexane (O_2) solubilized with a surfactant mixture of 100 mg Tween80 and 300 mg Span80 ($C^{O_2}_{T80}$= 5mM, $C^{O_2}_{S80}$ = 47 mM) to create the $O_1/W/O_2$ double nanoemulsion (ESI section I, Table S1). The mixture was subjected to 30 s of ultrasonication, divided into 4 batches of equal amount, and photocrosslinked at different time points over a period of 0 to 6 hours after ultrasonication.

We find that under these conditions, both the encapsulation efficiency and overall diameter of the nanogels remain relatively constant for waiting times up to 6 hours (Figure 4c). This indicates that the inner O_1 phase of the $O_1/W/O_2$ nanoemulsion is relatively stable toward coalescence with the outer O_2 phase after ultrasonication. Specifically, the stable size distribution suggests that little to no droplet ripening or coalescence occurs between $O_1/W/O_2$ droplets, and the stable encapsulation efficiency indicates no observable encapsulated oil loss. Therefore, we find that the instability of the $O_1/W/O_2$ nanoemulsions is dominated by the enhanced coalescence of the O_1 phase with the O_2 phase that occurs during the ultrasonication process (Scheme 1a).

To demonstrate that the $O_1/W/O_2$ templating method can be used to prepare nanogels with a wide range of crosslinking density, we studied the effect of PEGDA hydrogel pre-cursor concentration (ϕ_{PEGDA}^{W}) in the O_1/W nanoemulsion on oil encapsulation efficiency in the resulting nanogels. To prepare the samples, a silicone oil-in-water nanoemulsion of Φ^{O_1} = 0.10, ϕ_{PEGDA}^{W}= 0.33, C_{T20}^{W} = 117 mM was prepared, and the O_1/W nanoemulsion was then diluted to Φ^{O_1}= 0.04 with solutions containing different volume fractions of PEGDA in water to achieve final values of ϕ_{PEGDA}^{W} between 0.18 and 0.43 (ESI section I, Table S1). The average size of the silicone oil droplets in the O_1/W nanoemulsion after dilution (approximately 30 nm in all cases) was found to be independent of ϕ_{PEGDA}^{W} (ESI Table S2). These O_1/W nanoemulsions (Φ^{O_1}= 0.04) were then emulsified to make $O_1/W/O_2$ double nanoemulsions, polymerized to form nanogels, and the resulting oil encapsulation efficiency was quantified by NMR.

We observe a decrease in oil encapsulation efficiency with increasing ϕ_{PEGDA}^{W}, whereas the size of the nanogels remains relatively constant (Fig. 4d). The observed decrease in ε appears to occur above a threshold value of $\phi_{PEGDA}^{W} \sim 0.3$, below which the encapsulation

efficiency is relatively independent of PEGDA concentration. To confirm this result, cryo-TEM images for ϕ_{PEGDA}^{W} = 0.25 and 0.43 were taken of i) the $O_1/W/O_2$ nanoemulsions immediately after photocrosslinking, and ii) the final nanogels after purification and resuspension into water (Figure 5). The resulting images agree with the NMR results. Specifically, the images confirm that the nanogels at ϕ_{PEGDA}^{W} = 0.25 contain a large number of encapsulated oil nanodroplets, whereas the nanogels with ϕ_{PEGDA}^{W} = 0.43 do not have any discernable oil nanodroplets within them.

We can infer from the cryo-TEM images that the oil loss that occurs for ϕ_{PEGDA}^{W} = 0.43 does so prior to the photopolymerization process. Given the previous findings that ultrasonication significantly enhances droplet instability, this suggests that the presence of PEGDA in the $O_1/W/O_2$ nanoemulsions tends to enhance ultrasonication-induced droplet instability. We hypothesize that this is caused by the increased solubility of the surfactant Span80 in the aqueous phase with increasing ϕ_{PEGDA}^{W}, which we have verified by independent solubilization experiments (ESI Figure S1). It is likely that greater solubility of Span80 in the water/PEGDA (W) phase induces faster transfer of the Span80 molecule from the W/O_2 interface to the O_1/W interface, thereby lowering the interfacial tension at both interfaces[56] and facilitating the coalescence of inner oil droplets with the outer oil phase (Schematic 1b).

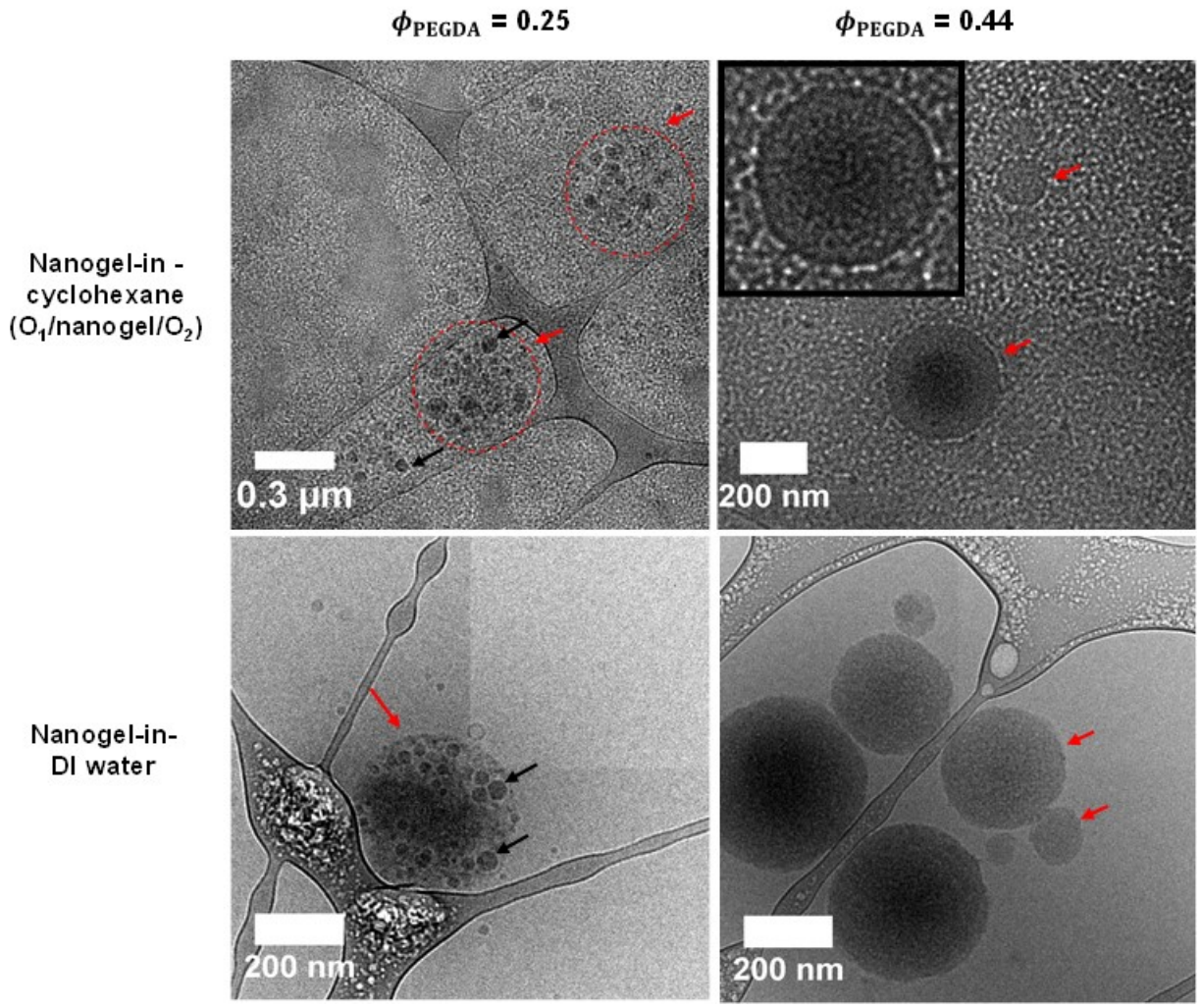

Figure 5. Cryo-TEM images comparing nanogels with Φ^{O_1}=0.04 at (left) ϕ^{W}_{PEGDA} = 0.25 and (right) ϕ^{W}_{PEGDA} = 0.43 both (top) immediately after crosslinking in the O_1/W/O_2 nanoemulsion, and (bottom) after purification into aqueous solution. In both cases, crosslinked nanogel particles are observed (red circles and red arrows), whereas small 30 nm silicone oil droplets were only observed for ϕ^{W}_{PEGDA} = 0.25 (black arrows).

Adaptability of double nanoemulsion nanogel synthesis to other materials

To further generalize the reported double nanoemulsion templating method for creating oil-laden nanogels, we tested the ability of the method to be used in templating nanogels containing other

oils and polymers. As shown in Figure 6a, the double nanoemulsion templating process is successful in creating PEGDA nanogels when the silicone oil is replaced with peanut oil nanodroplets with an average size of 20 nm. Moreover, this demonstrates that the oil-laden nanogels can be made entirely from biocompatible (non-toxic) components, facilitating their use for *in vivo* applications.

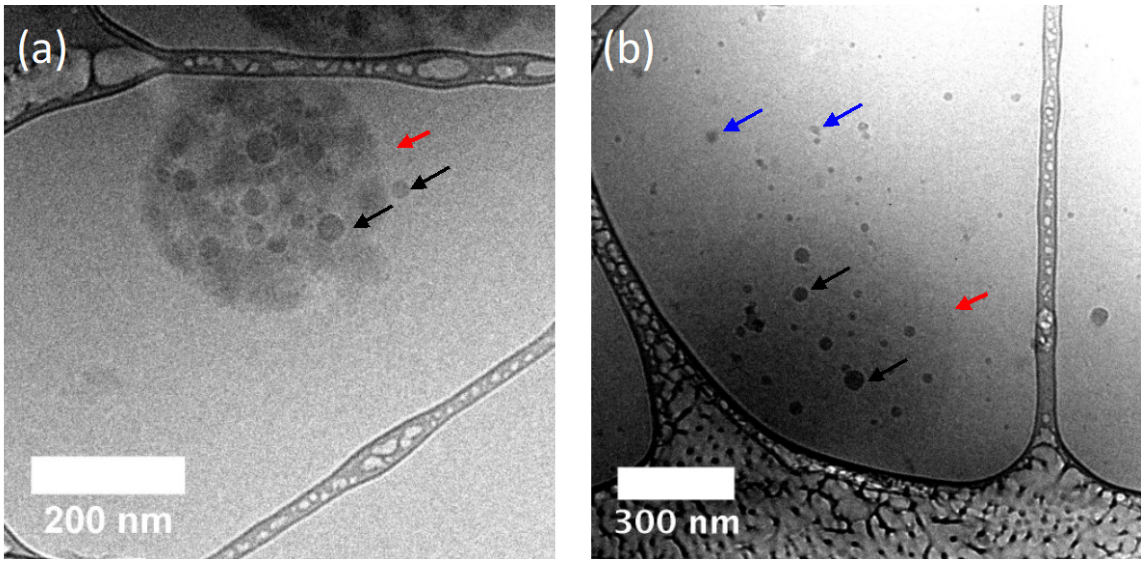

Figure 6. a) Cryo-TEM of nanogel (PEGDA, Mn=700) loaded with peanut oil droplets with the following composition: Φ^{O_1}=0.04, ϕ^{W}_{PEGDA}= 0.25, C^{W}_{T20} = 44 mM b) Cryo-TEM image of a nanogel with silicone oil as the inner phase and PEGDA (Mn = 10K) as the hydrogel precursor with the following composition: at $\Phi^{O_1} = 0.096, \phi^{W}_{PEGDA} = 0.2,$ and C^{W}_{SDS} = 222 mM; (red, black, blue arrows denote nanogel, oil droplets in nanogel, and oil loss to the surrounding, respectively).

As a demonstration that these oil-laden nanogels are non-toxic, a cytotoxicity assay was performed using MDA-MB-231 triple negative breast cancer cells (Figure 7), which indicates that these particles are relatively non-toxic for 24 hours (i.e. >80% of cells remain viable), which is comparable to or better than more widely studied drug nanocarriers at the same

concentrations.[57,58] More extensive studies of biological transport and toxicity are ongoing. However, we note that similar PEGDA nanogels without encapsulated oil droplets were previously studied by Anselmo et al., where studies of cellular uptake *in vitro* and biodistribution *in vivo* did not observe any adverse toxicity effects, and found that particles were cleared by the spleen.[25] In the case of oil-laden nanogels, we anticipate that the outside environment is only able to contact the nanogel, and not the encapsulated oil droplets. Thus, we expect oil-laden nanogels to have similar toxicity profiles and clearance mechanisms.

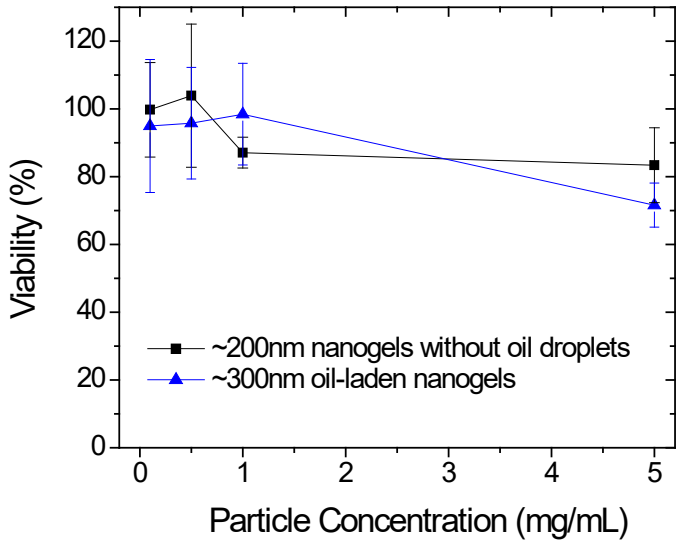

Figure 7. Toxicity of nanogels with and without oil on MDA-MB-231 triple negative breast cancer cells after 24 hour exposure. Viability was measured via MTT assay. Nanogels (black) have similar cell viability with (blue) and without (black) encapsulated oil nanodroplets.

This ease of altering the inner oil type is especially useful for delivery of anti-cancer drugs. More generally, vegetable oils (such as peanut oil, olive oil, soybean oil, *etc.*) are widely used to encapsulate hydrophobic drugs for drug delivery,[59–62] such as paclitaxel and camptothecin.[61,62] Given the known solubility of these drugs in a particular vegetable oil, the

total amount that can be encapsulated primarily depends on the encapsulation efficiency of oil droplets in the oil-laden nanogels.

We also tested whether the double nanoemulsion templating process is sensitive to replacing the relatively low molecular weight PEGDA macromer used in previous studies (M_n = 700 g/mol, PEGDA 700) with a macromer with significantly larger molecular weight (M_n = 10,000 g/mol, PEGDA 10k). This will have the effect of significantly increasing both the specific viscosity of the aqueous polymer phase during the nanoemulsification process, as well as the mesh size of the hydrogel network in the final nanogel particles. As shown in Figure 6b, we were successful in producing oil-laden nanogels with the larger PEGDA macromer (see SI Section I and Table S1 for composition and detailed process description). In this case, however, we found that the Tween20 surfactant was unable to produce sufficiently small silicone oil droplets in the O_1/W nanoemulsion, even after matching the viscosity ratio between the W and O_1 phases used for the shorter PEGDA macromer. Therefore, Tween20 was replaced with sodium dodecyl sulfate (SDS), which has a smaller packing parameter and is therefore capable of forming smaller nanoemulsion droplets.[55] Doing so, we produced sufficiently small oil nanodroplets for the formation of double nanoemulsions and subsequent formation of oil-laden nanogels (Figure 6b).

Upon purification of the nanogels and re-dispersion into water, cryo-TEM imaging indicates a significant loss of the oil nanodroplets from the nanogel interior, as evident by the appearance of oil nanodroplets surrounding the nanogel. This can be attributed to a combination of non-uniformity of nanogel crosslinking and the large swelling ratio Q of the 10,000 g/mol macromer in water. For bulk hydrogels at a concentration of ϕ^{W}_{PEGDA}=0.2, the swelling ratio is 3.56 for PEGDA 10k and 1.02 for PEGDA 700, which corresponds to an average mesh size of

16.3nm for PEGDA 10k and 3.1nm for PEGDA 700 in the swollen state.[63] Compared to the small mesh size of PEGDA 700, PEGDA 10k has an average mesh size that is comparable to the oil droplets, which would likely drive faster oil loss through the heterogeneous nanogel network.

Although this swelling behavior limits the oil encapsulation efficiency of particles produced from $O_1/W/O_2$ nanoemulsions for hydrogels with larger mesh size, it also demonstrates the intriguing possibility that hydrogel swelling can be used as a mechanism to induce release of the encapsulated nanodroplets from the nanogels. This provides a potential route to triggered release of nanodroplet cargoes (and actives encapsulated within them), and further studies toward this aim are ongoing.

CONCLUSION

We have developed a method for preparing $O_1/W/O_2$ nanoemulsions using sequential high-energy emulsification, and demonstrated its application for templating oil-laden polymer nanogels with controlled size, polymer density and encapsulated oil concentration. Given that production scale equipment for ultrasonication or closely related high-pressure homogenization already exists,[39,40] the method is eminently scalable, and provides a route to producing large quantities of multiple nanoemulsions, and multi-phase nanoparticles from them.

By characterizing the oil encapsulation efficiency across a range of processing parameters, we conclude that the primary mechanism of droplet instability in the double nanoemulsion is ultrasonication-enhanced coalescence of the inner O_1 phase with the outer O_2 phase due to rupture of the water film separating the two oil phases. This instability is enhanced

by the presence of PEGDA hydrogel pre-cursor, but only above a threshold concentration. Direct confirmation of this mechanism could be made by *in situ* monitoring of the inner oil phase, and is the subject of ongoing study. These results allow for the identification of processing conditions that optimize the oil encapsulation efficiency, which include relatively short ultrasonication times and low concentrations of inner oil and hydrogel precursor in the double nanoemulsion.

Optimizing the $O_1/W/O_2$ nanoemulsion stability results in double nanoemulsions with both inner and outer droplets that remain kinetically stable for many hours, facilitating their use as colloidal templates for multi-phase nanoparticles. Here, this was demonstrated through crosslinking and subsequent purification of oil-laden, water-swollen nanogels with relatively high encapsulation efficiency, with sizes ranging from 200-300 nm and relatively narrow size distribution and encapsulation polydispersity. The process is versatile to a range of nanogel compositions including the oil and polymer hydrogel chemistry, hydrogel crosslink density and encapsulated oil droplet size and concentration. Most significantly, we have demonstrated the ability to produce oil-laden nanogels entirely of commonly-used, biocompatible components. As such, we anticipate that the templating method and resulting nanogels will find use in a number of applications including pharmaceuticals, consumer products and foods.

METHODS

Synthesis of double nanoemulsions and templating of nanoparticles Poly(ethylene glycol) diacrylate (M_n = 700g/mol), Tween20, Tween80, Span80, cyclohexane (ACS reagent grade $\geq$ 99%), silicone oil (100 cSt), peanut oil, and 2-hydroxy-2-methylpropiophenone were purchased from Sigma Aldrich and used as received. Poly(ethylene glycol) diacrylate (M_n = 10,000g/mol)

was synthesized in our lab. PEG, 2.2 equiv of acryloyl chloride and trimethylamine reacted in dichloromethane for 8 h in a dark environment at room temperature. The solution was filtered and precipitated into ethyl ether. The product was collected by filtration and then dried in a vacuum oven prior to use. The molecular mass and molecular mass distribution were determined using a combination of ^{1}H NMR and GPC.

The double nanoemulsions and oil-laden nanoparticles were synthesized according to Figure 2a through a two-step high energy emulsification process. Emulsification by sonication was performed using a 700 Watt Fischer sonicator dismembrator with modular amplitude.

The standard protocol is as follows: First, an O_1/W pre-emulsion was created by dispersing an oil of interest (i.e. silicone oil) into a continuous phase consisting of water, poly(ethylene glycol) diacrylate, and Tween20. Unless otherwise stated, the typical stock composition for the O_1/W nanoemulsion is ϕ_{oil} = 0.10, ϕ_{PEGDA}^{W} = 0.33, C_{T20} = 117 mM. A high-energy ultrasonicator (Fisher Scientific Model FB705) was used to emulsify the pre-emulsion into 20-30 nm oil droplets using the pulse mode (pulse on: 5s, pulse off: 15s) and ice bath was used to minimize sample heating. At this point, the stock nanoemulsion was ready to be diluted down to a lower oil volume fraction with solutions containing either higher or lower concentrations of PEGDA to create suspensions with a wide range of ϕ_{PEGDA}^{W}. Detailed recipes for O_1/W nanoemulsion for each figure can be found in ESI. In the particular sample shown in Figure 2, the stock O_1/W was diluted with pure ϕ_{PEGDA}= 0.20 solution to get a final composition of ϕ_{oil} =0.04, and ϕ_{PEGDA}^{W} = 0.25, C_{T20}^{W} = 44 mM. 1 mL of this O_1/W nanoemulsion was then dispersed into 15 mL of an outer oil O_2 (cyclohexane) phase with 300 mg of Span80 and 100 mg of Tween80 and let stir for 30 minutes at speed of 500 rpm. The pre-emulsion was then ultrasonicated for 30 s to 1 minute at an amplitude of 30% (32 Watt) using pulse mode (pulse on:

5s, pulse off: 5s) to a final size of 300 nm. An ice bath was again employed to minimize sample heating. 100 μL of photoinitiator 2-hydroxy-2-methylpropiophenone was then added to the sample and the sample was UV-polymerized *via* free-radical polymerization for 5 min using a 365 nm long-wave UV lamp. The nanoparticles were then washed first in cyclohexane *via* centrifugation (20 mL, 1 round, 18,000g), then in DI water (35 mL, 2 rounds, 25,000g), and then re-suspended in DI water. Nanoparticle concentrations can be determined by freeze-drying a known volume and measuring the freeze-dried mass.

For experimental purposes, the multiple nanoemulsions and resulting particles are prepared in batches of 15 mL. However, using our bench-scale ultrasonicator, this can easily scale up to as much as 250 mL. For larger batches or continuous processing, industrial scale ultrasonicators also exist,[39,40] and are demonstrated to produce quantities up to 10L. Alternatively, high-pressure homogenizers can be used to produce emulsions on a large scale in a continuous fashion. For example, such scalable production has already been demonstrated for O_1/W nanoemulsions studied in this work.[21]

Particle Size. Size measurements were obtained by dynamic light scattering (DLS) using a BI-20S (Brookhaven Instruments) with a HeNe 632 nm laser with multi-angle capabilities. Measurements were carried out at 20 ºC and a fixed angle of 90 degrees. Autocorrelation functions were collected and fit to a cumulant analysis to obtain the Z-average and polydispersity index (PDI). All nanoemulsions were diluted to a final concentration of <1 wt% and remain optically transparent during DLS measurements. The crosslinked nanogel particles were diluted with Millipore DI water to ~0.01 wt% by dry mass, such that the scattering intensity was maintained around 200-500 kcps for all measurements.

Particle Structure. *Cryogenic Transmission Electron Microscopy (Cryo-TEM)* was used to decipher the internal structure of both the double nanoemulsion and the oil-laden nanogels. Samples were prepared using a Vitrobot Mark IV at room temperature and variable humidity (100% RH for aqueous sample, no humidity control for organic phase samples). Lacey carbon coated copper grids (200 mesh) were acquired from Electron Microscopy Sciences and used as the sample grid for both aqueous and organic phase (i.e. cyclohexane) samples. For aqueous phase samples, the grids were plasma-treated for 20 seconds prior to vitrification in liquid ethane for aqueous samples. For organic phase samples (i.e. samples in cyclohexane), the grids were used directly without plasma treatment and liquid nitrogen was selected as the vitrifying liquid. The procedure for sample preparation is as follows: first, 1.2 μL of aqueous phase samples (2 μL for organic phase) was deposited onto the grid; the grid was then blotted to remove excess liquid (blotting time: 1s, blotting force: 2, number of blots: 1), and subsequently plunged into the vitrifying liquid to trap the sample in a thin layer of amorphous ice. The samples were then transferred to the cryo-TEM holder and viewed under the FEI Tecnai G2 Sphera TEM at 200kV. Low-dose mode was used for organic phase samples. Gatan Digital Micrograph was used to record the images acquired by the digital camera.

Particle oil content. Solid-state ^{1}H NMR was used to analyze the oil content of the oil-laden nanogels. For sample preparation, the washed nanogel particles were dispersed in D_2O and spun down into a pellet. The pellet was then diluted by adding a small amount of D_2O and placed into a 50 uL NMR rotor with a Kel-F cap. The rotor was then placed into a solid-state 500 MHz NMR (Bruker Avance IPSO500) and spun at a speed of 8 kHz.

MTT assay. To assess toxicity, cells were seeded in 96-well cell culture plates at a density of 10,000 cells per well and allowed to adhere overnight. Media was then replaced with fresh media

containing various concentrations of nanoparticles and incubated for 24 hours. The nanoparticle solution was subsequently removed and replaced with 0.5 mg/mL 3-(4,5-Dimethylthiazol-2-yl)-2,5-diphenyltetrazolium bromide (MTT) in media. After 4 hours, MTT solution was aspirated and replaced with dimethylsulfoxide (DMSO) to solubilize the formazan crystals that result from intracellular reduction of MTT. Absorbance at 570nm was measured using a Tecan Infinite M200 Pro plate reader (Männedorf, Switzerland) to determine dye intensity. Viability is reported relative to an untreated control group.

ASSOCIATED CONTENT

Supporting Information. This document is available free of charge. Detailed protocol for nanogel fabrication for Figure 2, 4, 6 (Section I, Table S1). Solubility of PEGDA in Span 80 (Figure S1). Additional cryo-TEM images of nanogels (Figure S2). Additional DLS data on O/W nanoemulsion (Table S2). Stability data on oil encapsulation (Table S3). Swelling ratio of PEGDA 10,000g/mol and 700g/mol (Table S4).

AUTHOR INFORMATION

Corresponding Author

* helgeson@engineering.ucsb.edu

Author Contributions

MZ, MN, PMdM and MEH designed the experiments; MZ, MN, MA and KS carried out the experiments. MZ, MN, MEH, and SM prepared the manuscript. All authors have given approval to the final version of the manuscript.

ACKNOWLEDGMENTS

MZ was funded in part by the University of California Cancer Research Coordinating Committee under award number CRC-15-380521, 20150630 and by the Hellman Foundation. MN was funded by the National Science Foundation Graduate Research Fellowship Program under Grant No. DGE-1144085. PMdM was funded by the Defense Threat Reduction Agency under the Natick Soldier Research, Development and Engineering Center Agreement No. W911QY-13-2-0001. The MRL Shared Experimental Facilities are supported by the MRSEC Program of the NSF under Award No. DMR-1121053; a member of the NSF-funded Materials Research Facilities Network (www.mrfn.org). We thank Jerry Hu for assistance during the solid state NMR experiments as well as Frank Polzer and Stephan Kraemer for cryo-TEM training.

ABBREVIATIONS

PEGDA, poly(ethylene glycol) diacrylate; DLS, dynamic light scattering, NMR, nuclear magnetic resonance; cryo-TEM, cryogenic transmission electron microscopy; W/O/W water-in-oil-in-water; O/W/O oil-in-water-in-oil.

REFERENCES

(1) Zeeb, B.; Saberi, A. H.; Weiss, J.; McClements, D. J. Retention and Release of Oil-in-Water Emulsions from Filled Hydrogel Beads Composed of Calcium Alginate: Impact of Emulsifier Type and pH. *Soft Matter* **2015**, *11*, 2228–2236. doi: 10.1039/c4sm02791d

(2) Matalanis, A.; Jones, O. G.; McClements, D. J. Structured Biopolymer-Based Delivery Systems for Encapsulation, Protection, and Release of Lipophilic Compounds. *Food Hydrocoll.* **2011**, *25*, 1865–1880. doi: 10.1016/j.foodhyd.2011.04.014

(3) Muschiolik, G. Multiple Emulsions for Food Use. *Curr. Opin. Colloid Interface Sci.* **2007**, *12*, 213–220. doi: 10.1016/j.cocis.2007.07.006

(4) Sapei, L.; Naqvi, M. A.; Rousseau, D. Stability and Release Properties of Double Emulsions for Food Applications. *Food Hydrocoll.* **2012**, *27*, 316–323. doi: 10.1016/j.foodhyd.2011.10.008

(5) Yu, S. C.; Bochot, A.; Le Bas, G.; Chéron, M.; Mahuteau, J.; Grossiord, J. L.; Seiller, M.; Duchêne, D. Effect of Camphor/cyclodextrin Complexation on the Stability of O/W/O Multiple Emulsions. *Int. J. Pharm.* **2003**, *261*, 1–8. doi: 10.1016/s0378-5173(03)00261-8

(6) Laugel, C.; Baillet, A.; Youenang Piemi, M. P.; Marty, J. P.; Ferrier, D. Oil-Water-Oil Multiple Emulsions for Prolonged Delivery of Hydrocortisone after Topical Application: Comparison with Simple Emulsions. *Int. J. Pharm.* **1998**, *160*, 109–117. doi: 10.1016/s0378-5173(97)00302-5

(7) Mishra, B.; Pandit, J. K. Prolonged Release of Pentazocine from Multiple O/W/O Emulsions. *Drug Dev. Ind. Pharm.* **1989**, *15*, 1217–1230. doi: 10.3109/03639048909043673

(8) Okochi, H.; Nakano, M. Preparation and Evaluation of W/o/w Type Emulsions Containing Vancomycin. *Advanced Drug Delivery Reviews*, 2000, *45*, 5–26. doi: 10.1016/s0169-409x(00)00097-1

(9) Onuki, Y.; Morishita, M.; Takayama, K. Formulation Optimization of Water-in-Oil-Water Multiple Emulsion for Intestinal Insulin Delivery. *J. Control. Release* **2004**, *97*, 91–99. doi: 10.1016/j.jconrel.2004.03.010

(10) Lindenstruth, K.; Müller, B. W. W/O/W Multiple Emulsions with Diclofenac Sodium. *Eur. J. Pharm. Biopharm.* **2004**, *58*, 621–627. doi:10.1016/j.ejpb.2004.04.003

(11) Miyazawa, K.; Yajima, I.; Kaneda, I.; Yanaki, T. Preparation of a New Soft Capsule for Cosmetics. *J. Cosmet. Sci.* **2000**, *51*, 239–252.

(12) Zatz, J. L.; Cueman, G. H. Assessment of Stability in Water-in-Oil-in-Water Multiple Emulsions. *J. Soc. Cosmet. Chem.* **1988**, *39*, 211–222.

(13) Lee, J.-S.; Kim, J.-W.; Han, S.-H.; Chang, I.-S.; Kang, H.-H.; Lee, O.-S.; Oh, S.-G.; Suh, K.-D. The Stabilization of L-Ascorbic Acid in Aqueous Solution and Water-in-Oil-in-Water Double Emulsion by Controlling pH and Electrolyte Concentration. *J. Cosmet. Sci.* **2004**, *55*, 1–12. doi: 10.1111/j.0142-5463.2004.00223_1.x

(14) Chakraborty, M.; Bart, H.-J. Emulsion Liquid Membranes: Role of Internal Droplet Size Distribution on Toluene/n-Heptane Separation. *Colloids Surfaces A Physicochem. Eng. Asp.* **2006**, *272*, 15–21. doi: 10.1016/j.colsurfa.2005.07.002

(15) Kawasaki, J.; Kosuge, H.; Egashira, R.; Asawa, T. Mechanical Entrainment in W/O/W Emulsion Liquid Membrane. *Sep. Sci. Technol.* **2009**, *44*, 151–168. doi: 10.1080/01496390802437115

(16) Gupta, S.; Chakraborty, M.; Murthy, Z. V. P. Removal of Mercury by Emulsion Liquid Membranes: Studies on Emulsion Stability and Scale Up. *J. Dispers. Sci. Technol.* **2013**, *34*, 1733–1741. doi: 10.1080/01932691.2013.767205

(17) Hoare, T. R.; Kohane, D. S. Hydrogels in Drug Delivery: Progress and Challenges. *Polymer (Guildf).* **2008**, *49*, 1993–2007. doi: 10.1016/j.polymer.2008.01.027

(18) Hamidi, M.; Azadi, A.; Rafiei, P. Hydrogel Nanoparticles in Drug Delivery. *Adv. Drug*

Deliv. Rev. **2008**, *60*, 1638–1649. doi: 10.1016/j.addr.2008.08.002

(19) Gawande, M. B.; Goswami, A.; Asefa, T.; Guo, H.; Biradar, A. V; Peng, D.; Zboril, R.; Varma, R. S. Core-Shell Nanoparticles: Synthesis and Applications in Catalysis and Electrocatalysis. *Chem. Soc. Rev.* **2015**, *44*, 7540–7590. doi: 10.1039/c5cs00343

(20) Son, S.; Hwang, S. H.; Kim, C.; Yun, J. Y.; Jang, J. Designed Synthesis of SiO 2 /TiO 2 Core/Shell Structure As Light Scattering Material for Highly Efficient Dye-Sensitized Solar Cells. *ACS Appl. Mater. Interfaces* **2013**, *5*, 4815–4820. doi: 10.1021/am400441v

(21) Helgeson, M. E.; Moran, S. E.; An, H. Z.; Doyle, P. S. Mesoporous Organohydrogels from Thermogelling Photocrosslinkable Nanoemulsions. *Nat. Mater.* **2012**, *11*, 344–352. doi: 10.1038/nmat3248

(22) An, H. Z.; Helgeson, M. E.; Doyle, P. S. Nanoemulsion Composite Microgels for Orthogonal Encapsulation and Release. *Adv. Mater.* **2012**, *24*, 3838–3844, 3895. doi: 10.1002/adma.201200214

(23) Singh, R.; Lillard, J. W. Nanoparticle-Based Targeted Drug Delivery. *Exp. Mol. Pathol.* **2009**, *86*, 215–223. doi: 10.1016/j.yexmp.2008.12.004

(24) Chacko, R. T.; Ventura, J.; Zhuang, J.; Thayumanavan, S. Polymer Nanogels: A Versatile Nanoscopic Drug Delivery Platform. *Adv. Drug Deliv. Rev.* **2012**, *64*, 836–851. doi: 10.1016/j.addr.2012.02.002

(25) Anselmo, A. C.; Zhang, M.; Kumar, S.; Vogus, D. R.; Menegatti, S.; Helgeson, M. E.; Mitragotri, S. Elasticity of Nanoparticles Influences Their Blood Circulation,

Phagocytosis, Endocytosis, and Targeting. *ACS Nano* **2015**, *9*, 3169–3177. doi: 10.1021/acsnano.5b00147

(26) An, H. Z.; Safai, E. R.; Burak Eral, H.; Doyle, P. S. Synthesis of Biomimetic Oxygen-Carrying Compartmentalized Microparticles Using Flow Lithography. *Lab Chip* **2013**, *13*, 4765–4774. doi: 10.1039/c3lc50610j

(27) Abate, A. R.; Weitz, D. A. High-Order Multiple Emulsions Formed in Poly(dimethylsiloxane) Microfluidics. *Small* **2009**, *5*, 2030–2032. doi: 10.1002/smll.200900569

(28) Utada, A. S.; Lorenceau, E.; Link, D. R.; Kaplan, P. D.; Stone, H. A.; Weitz, D. A. Monodisperse Double Emulsions Generated from a Microcapillary Device. *Science* **2005**, *308*, 537–541. doi: 10.1126/science.1109164

(29) Kim, S.-H.; Nam, J.; Kim, J. W.; Kim, D.-H.; Han, S.-H.; Weitz, D. a. Formation of Polymersomes with Double Bilayers Templated by Quadruple Emulsions. *Lab Chip* **2013**, *13*, 1351–1356. doi: 10.1039/c3lc41112e

(30) Arriaga, L. R.; Datta, S. S.; Kim, S.-H.; Amstad, E.; Kodger, T. E.; Monroy, F.; Weitz, D. A. Ultrathin Shell Double Emulsion Templated Giant Unilamellar Lipid Vesicles with Controlled Microdomain Formation. *Small* **2014**, *10*, 950–956. doi: 10.1002/smll.201301904

(31) Arriaga, L. R.; Amstad, E.; Weitz, D. A. Scalable Single-Step Microfluidic Production of Single-Core Double Emulsions with Ultra-Thin Shells. *Lab Chip* **2015**, *15*, 3335–3340. doi: 10.1039/c5lc00631g

(32) Clegg, P. S.; Tavacoli, J. W.; Wilde, P. J. One-Step Production of Multiple Emulsions: Microfluidic, Polymer-Stabilized and Particle-Stabilized Approaches. *Soft Matter* **2016**, *12*, 998–1008. doi: 10.1039/c5sm01663k

(33) Besnard, L.; Marchal, F.; Paredes, J. F.; Daillant, J.; Pantoustier, N.; Perrin, P.; Guenoun, P. Multiple Emulsions Controlled by Stimuli-Responsive Polymers. *Adv. Mater.* **2013**, *25*, 2844–2848. doi: 10.1002/adma.201204496

(34) Thompson, K. L.; Mable, C. J.; Lane, J. A.; Derry, M. J.; Fielding, L. A.; Armes, S. P. Preparation of Pickering Double Emulsions Using Block Copolymer Worms. *Langmuir* **2015**, *31*, 4137–4144. doi: 10.1021/acs.langmuir.5b00741

(35) Pradhan, M.; Rousseau, D. A One-Step Process for Oil-in-Water-in-Oil Double Emulsion Formation Using a Single Surfactant. *J. Colloid Interface Sci.* **2012**, *386*, 398–404. doi: 10.1016/j.jcis.2012.07.055

(36) Mezzenga, R.; Folmer, B. M.; Hughes, E. Design of Double Emulsions by Osmotic Pressure Tailoring. *Langmuir* **2004**, *20*, 3574–3582. doi: 10.1021/la036396k

(37) Hong, L.; Sun, G.; Cai, J.; Ngai, T. One-Step Formation of W/O/W Multiple Emulsions Stabilized by Single Amphiphilic Block Copolymers. *Langmuir* **2012**, *28*, 2332–2336. doi: 10.1021/la205108w

(38) Silva, B. F. B.; Rodríguez-Abreu, C.; Vilanova, N. Recent Advances in Multiple Emulsions and Their Application as Templates. *Curr. Opin. Colloid Interface Sci.* **2016**, *25*, 98–108. doi: 10.1016/j.cocis.2016.07.006

(39) Peshkovsky, A. S.; Bystryak, S. Continuous-Flow Production of a Pharmaceutical Nanoemulsion by High-Amplitude Ultrasound: Process Scale-Up. *Chem. Eng. Process. Process Intensif.* **2014**, *82*, 132–136. doi: 10.1016/j.cep.2014.05.007

(40) Peshkovsky, S. L.; Peshkovsky, A. S. High Capacity Ultrasonic Reactor System. U.S. Patent 8,651,230 B2, February 18, 2014.

(41) Shakeel, F.; Haq, N.; Al-Dhfyan, A.; Alanazi, F. K.; Alsarra, I. A. Double W/o/w Nanoemulsion of 5-Fluorouracil for Self-Nanoemulsifying Drug Delivery System. *J. Mol. Liq.* **2014**, *200*, 193–190. doi: 10.1016/j.molliq.2014.10.013

(42) Lee, H. S.; Morrison, E. D.; Zhang, Q.; McCormick, A. V. Cryogenic Transmission Electron Microscopy Study: Preparation of Vesicular Dispersions by Quenching Microemulsions. *J. Microsc.* **2016**, *263*, 293–299. doi: 10.1111/jmi.12392

(43) Malo de Molina, P.; Zhang, M.; Bayles, A.; Helgeson, M. E. Oil-in-Water-in-Oil Multi-Nanoemulsions for Templating Complex Nanoparticles. *Nano Lett.* **2016**. doi: 10.1021/acs.nanolett.6b02073

(44) Zhao, Y.; Zhang, J.; Wang, Q.; Li, J.; Han, B. Water-in-Oil-in-Water Double Nanoemulsion Induced by CO(2). *Phys. Chem. Chem. Phys.* **2011**, *13*, 684–689. doi: 10.1039/c0cp00869a

(45) Lee, H. S.; Morrison, E. D.; Frethem, C. D.; Zasadzinski, J. A.; McCormick, A. V. Cryogenic Electron Microscopy Study of Nanoemulsion Formation from Microemulsions. *Langmuir* **2014**, *30*, 10826–10833. doi: 10.1021/la502207f

(46) Porras, M.; Solans, C.; González, C.; Martínez, A.; Guinart, A.; Gutiérrez, J. M. Studies of Formation of W/O Nano-Emulsions. *Colloids Surfaces A Physicochem. Eng. Asp.* **2004**, *249*, 115–118. doi: 10.1016/j.colsurfa.2004.08.060

(47) Helgeson, M. E. Colloidal Behavior of Nanoemulsions: Interactions, Structure and Rheology. *Curr. Opin. Colloid Interface Sci.* **2016**, *25*, 39–50. doi: 10.1016/j.cocis.2016.06.006

(48) Gupta, A.; Eral, H. B.; Hatton, T. A.; Doyle, P. S. Nanoemulsions: Formation, Properties and Applications. *Soft Matter* **2016**, *12*, 2826–2841. doi: 10.1039/c5sm02958a

(49) McClements, D. J. Edible Nanoemulsions: Fabrication, Properties, and Functional Performance. *Soft Matter* **2011**, *7*, 2297. doi: 10.1039/c0sm00549e

(50) Pays, K.; Giermanska-Kahn, J.; Pouligny, B.; Bibette, J.; Leal-Calderon, F. Coalescence in Surfactant-Stabilized Double Emulsions. *Langmuir* **2001**, *17*, 7758–7769. doi: 10.1021/la010735x

(51) Pays, K.; Giermanska-Kahn, J.; Pouligny, B.; Bibette, J.; Leal-Calderon, F. Double Emulsions: How Does Release Occur? *J. Control. Release* **2002**, *79*, 193–205. doi: 10.1016/s0168-3659(01)00535-1

(52) Ficheux, M.; Bonakdar, L.; Bibette, J. Some Stability Criteria for Double Emulsions. *Langmuir* **1998**, *14*, 2702–2706. doi: 10.1021/la971271z

(53) Nollet, M.; Mercé, M.; Laurichesse, E.; Pezon, A.; Soubabère, O.; Besse, S.; Schmitt, V. Water Fluxes and Encapsulation Efficiency in Double Emulsions: Impact of

Emulsification and Osmotic Pressure Unbalance. *Soft Matter* **2016**, *12*, 3412–3424. doi: 10.1039/c5sm03089g

(54) Van Der Graaf, S.; Schroën, C. G. P. H.; Boom, R. M. Preparation of Double Emulsions by Membrane Emulsification - A Review. *J. Memb. Sci.* **2005**, *251*, 7–15. doi: 10.1016/j.memsci.2004.12.013

(55) Wooster, T. J.; Golding, M.; Sanguansri, P. Impact of Oil Type on Nanoemulsion Formation and Ostwald Ripening Stability. *Langmuir* **2008**, *24*, 12758–12765. doi: 10.1021/la801685v

(56) Hashimoto, M.; Garstecki, P.; Stone, H. A.; Whitesides, G. M. Interfacial Instabilities in a Microfluidic Hele-Shaw Cell. *Soft Matter* **2008**, *4*, 1403. doi: 10.1039/b715867j

(57) Grabowski, N.; Hillaireau, H.; Vergnaud, J.; Santiago, L. A.; Kerdine-Romer, S.; Pallardy, M.; Tsapis, N.; Fattal, E. Toxicity of Surface-Modified PLGA Nanoparticles toward Lung Alveolar Epithelial Cells. *Int. J. Pharm.* **2013**, *454*, 686–694. doi: 10.1016/j.ijpharm.2013.05.025

(58) Abbasalipourkabir, R.; Salehzadeh, A.; Abdullah, R. Cytotoxicity Effect of Solid Lipid Nanoparticles on Human Breast Cancer Cell Lines. *Biotechnology* **2011**, *10*, 528–533. doi: 10.3923/biotech.2011.528.533

(59) Khuphe, M.; Mukonoweshuro, B.; Kazlauciunas, A.; Thornton, P. D. A Vegetable Oil-Based Organogel for Use in pH-Mediated Drug Delivery. *Soft Matter* **2015**, *11*, 9160–9167. doi: 10.1039/c5sm02176f

(60) Singh, V.; Sagiri, S.; Pramanik, K.; Anis, A.; Ray, S.; Banerjee, I.; Pal, K. Vegetable Oil–Based Formulations for Controlled Drug Delivery. In *Handbook of Encapsulation and Controlled Release*; CRC Press, 2015; pp. 1381–1411.

(61) Chung, H.; Jeong, S. Y.; Kwon, I. C.; Park, Y. T.; Lee, I. H.; Yuk, S. H.; Choi, Y. W.; Park, J. H.; Chung, J. W. Composition for Solubilization of Paclitaxel and Preparation Method Thereof, U.S. Patent 8,075,917 B2, Dec 13, 2011.

(62) Wall, M. E.; Wani, M. C.; Manikumar, G.; Balasubramanian, N.; Vyas, D. Camptothecin β-Alanine Esters with Topoisomerase I Inhibition, U.S. Patent 6,288,072 B1, Sept 11, 2001.

(63) Malo de Molina, P.; Lad, S.; Helgeson, M. E. Heterogeneity and Its Influence on the Properties of Difunctional Poly(ethylene Glycol) Hydrogels: Structure and Mechanics. *Macromolecules* **2015**, *48*, 5402–5411. doi: 10.1021/acs.macromol.5b01115

For Table of Contents Use Only

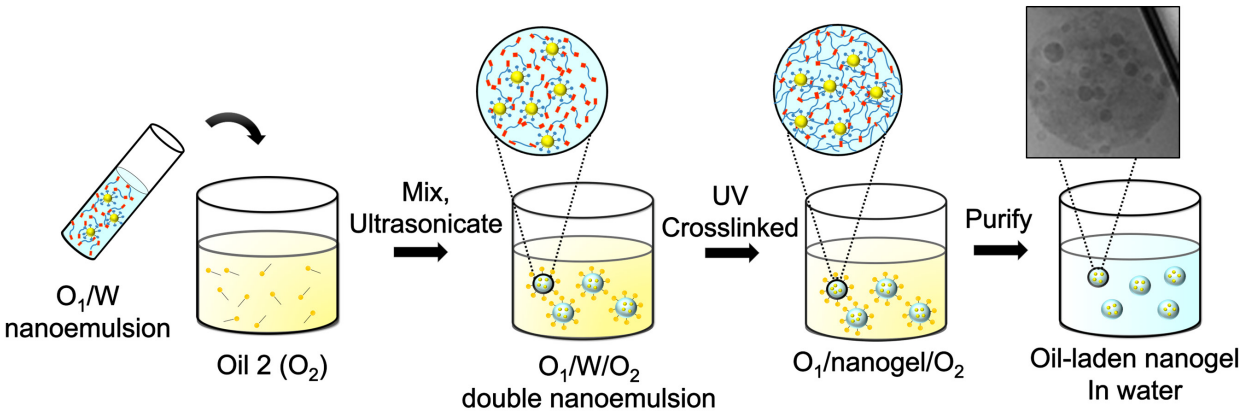

TOC Graphic. Sequential emulsification enables the controlled preparation of O/W/O multiple nanoemulsions, which can be used as templates for multi-compartment nanogel capsules.